



## Reactive additives for alkali capture in biomass combustion

Wu, Hao; Wang, Guoliang; Jensen, Peter Arendt; Jappe Frandsen, Flemming; Glarborg, Peter

*Publication date:*  
2018

*Document Version*  
Peer reviewed version

[Link back to DTU Orbit](#)

*Citation (APA):*

Wu, H., Wang, G., Jensen, P. A., Jappe Frandsen, F., & Glarborg, P. (2018). *Reactive additives for alkali capture in biomass combustion*. Paper presented at 27th International Conference on the Impact of Fuel Quality on Power Production and the Environment, Lake Louise, Alberta, Canada.

---

### General rights

Copyright and moral rights for the publications made accessible in the public portal are retained by the authors and/or other copyright owners and it is a condition of accessing publications that users recognise and abide by the legal requirements associated with these rights.

- Users may download and print one copy of any publication from the public portal for the purpose of private study or research.
- You may not further distribute the material or use it for any profit-making activity or commercial gain
- You may freely distribute the URL identifying the publication in the public portal

If you believe that this document breaches copyright please contact us providing details, and we will remove access to the work immediately and investigate your claim.

# Reactive Additives for Alkali Capture in Biomass Combustion

*Hao Wu\*, Guoliang Wang, Peter Arendt Jensen, Flemming Jappe Frandsen, Peter Glarborg*

Department of Chemical and Biochemical Engineering, Technical University of Denmark,  
Søltofts Plads 229, 2800 Kgs. Lyngby, Denmark

\*haw@kt.dtu.dk

## ABSTRACT

Biomass, as a renewable and CO<sub>2</sub> neutral fuel, is combusted in fluidized bed, grate and pulverized fuel-fired boilers for heat and power production. The gaseous alkali species released from biomass combustion, such as KCl and KOH, can cause several operation problems in the boilers, including ash deposition, corrosion, bed agglomeration, and deactivation of SCR catalysts. To address these problems, reactive additives that can convert the harmful gaseous alkali species to less harmful species, have been studied extensively through experiments and modelling. This paper aims to provide a discussion of the current understanding and applications of reactive additives for alkali capture in biomass combustion. The focus is on the thermodynamics, reaction mechanism, kinetics, and application aspects of sulfur based additives and Al-Si based additives.

## 1. INTRODUCTION

Combustion technologies, including fluidized bed combustion, grate combustion and pulverized fuel (PF) combustion, are used extensively for heat and power production from biomass. A common challenge for the utilization of biomass through the different combustion technologies is the operation problems induced by biomass ash, such as ash deposition and corrosion on boiler heat exchange surfaces,<sup>1</sup> deactivation of the catalyst for the selective catalytic reduction (SCR) unit,<sup>2</sup> and bed agglomeration in fluidized bed boilers.<sup>3</sup>

The ash-related operation problems are caused primarily by the potassium present in biomass. Typically, herbaceous biomass has relatively high concentrations of potassium (K), chlorine (Cl) and silicon (Si), which can form potassium chloride (KCl) and potassium silicates during combustion.<sup>4</sup> The low-melting temperature of KCl and the low viscosity of potassium silicates can lead to ash deposition problems in boilers, especially at the superheater region, and the deposited KCl can corrode the superheater surfaces.<sup>5</sup> Besides, the aerosols generated from the gaseous potassium species in the flue gas can deactivate the vanadium based SCR catalyst through both physical blocking and chemical poisoning.<sup>2</sup> Compared to herbaceous biomass, woody biomass has often much lower concentrations of K, Cl and Si. However, due to the high volatility of potassium in woody biomass,<sup>6</sup> a considerable amount of gaseous potassium species,

such as KCl and potassium hydroxide (KOH), can still be formed during combustion, leading to ash deposition, corrosion and SCR catalyst deactivation problems in boilers.<sup>7,8</sup>

The most common countermeasures for ash-related operation problems in biomass combustion include:

- Co-firing of biomass with a secondary fuel (such as coal) that can positively affect the ash chemistry during combustion.<sup>9</sup>
- Pretreatment of biomass (such as washing<sup>10</sup> and torrefaction<sup>11</sup>) to reduce the concentrations of alkali and chlorine in biomass.
- Modification of boiler design and operations (such as placing the SCR unit downstream of the electrostatic precipitator of a boiler)
- Utilization of additives that can convert the harmful alkali species into less harmful species.

Compared to other countermeasures, utilization of additives has several advantages, such as high-efficiency, low-capital cost, easy and fast implementation, and less-dependence on the policy regarding the fuels that can be fired/co-fired in boilers. Additives for capturing gaseous alkali species from biomass combustion have been studied extensively through experiments and modelling. Industrial application has been available in some biomass-fired boilers. For example, in a biomass PF-fired plant in Denmark, coal fly ash is used to capture the gaseous potassium (mainly KCl and KOH) released from pulverized wood combustion, with the ash deposition, corrosion and SCR deactivation problems mitigated.<sup>7,8</sup>

This review aims to provide a discussion of the current understanding and applications of using reactive additives for mitigating ash related operation problems in biomass combustion. The focus is on sulfur based additives and Al-Si based additives, primarily based on the research carried out at Technical University of Denmark. The additives that do not react with the alkali species are not discussed in this review.

## 2. CLASSIFICATION OF ADDITIVES

The reactive additives that are applicable to address ash related operation problems in biomass combustion are summarized in Table 1. They are classified according to the major active elements in them.

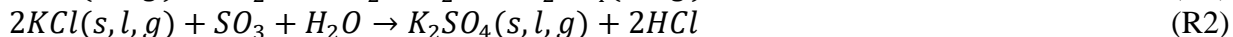
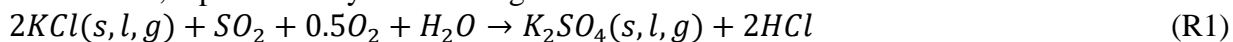
Table 1 Common additives for ash related operation problems in biomass combustion. The table is modified from the work of Jensen et al.<sup>12</sup>

Type	Species
Sulfur based additives	Sulfur dioxide, <sup>13–16</sup> elemental sulfur, <sup>17–19</sup> ammonium sulfate, <sup>19–24</sup> ferric sulfate, <sup>17,25</sup> aluminum sulfate, <sup>25</sup> sulfuric acid <sup>26</sup>
Al-Si based additives	Kaolin, <sup>27–34</sup> mullite, <sup>30–32</sup> coal fly ash, <sup>7,8,34</sup> spent bleaching earth, <sup>27</sup> bentonite, <sup>35</sup> sand, <sup>35</sup> bauxite, <sup>34</sup> clay, <sup>22</sup> emathlite <sup>36</sup>
Phosphorous based additives*	Monocalcium phosphate, <sup>22</sup> calcium phosphate, <sup>37</sup> di-ammonium phosphate, <sup>38</sup> mono-ammonium phosphate <sup>38</sup>

\* Phosphorous based additives are not covered in this review.

### 3. SULFUR BASED ADDITIVES

The main working principle of the sulfur based additives is sulfation of alkali chlorides to alkali sulfates, represented by the follow global reactions:



The melting temperature of  $K_2SO_4$  (1069 °C) is considerably higher than that of  $KCl$  (770 °C), and  $K_2SO_4$  is much less corrosive compared to  $KCl$ . Thus, sulfation of alkali chlorides can mitigate ash deposition and corrosion problems in boilers. However,  $K_2SO_4$  can still lead to deactivation of the vanadium based SCR catalyst.<sup>39</sup>

#### 3.1 Thermodynamics of K-S-Cl system

The thermodynamics of a typical K-S-Cl system is evaluated through global equilibrium calculation, based on a simulated flue gas containing 5%  $O_2$ , 10%  $CO_2$ , 15%  $H_2O$ , 200 ppm K, 100 ppm Cl and 200 ppm S (balanced by  $N_2$ ). The distribution of the K species in the temperature range of 600-1500 °C is shown in Figure 1.  $KOH(g)$  and  $KCl(g)$  are the thermodynamically favorable K species at temperatures above 1300 °C. The formation of  $K_2SO_4$  becomes thermodynamically feasible when the temperature is below 1300 °C, and the amount of  $K_2SO_4$  increases with decreasing temperatures. Below 800 °C,  $K_2SO_4$  is the only thermodynamically favorable K species under the studied conditions.

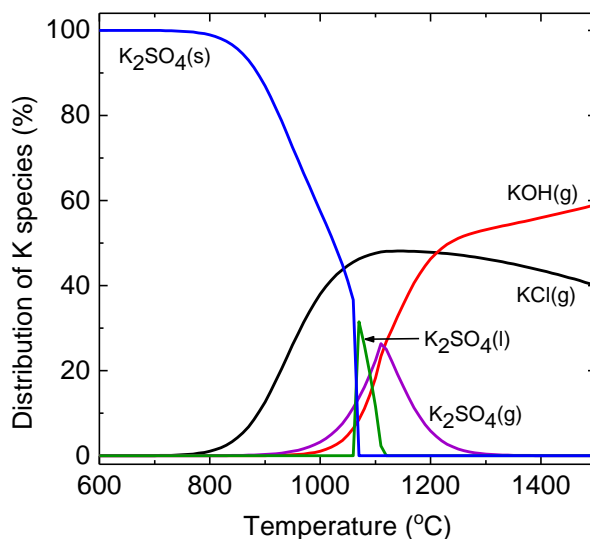


Figure 1 Distribution of K species from global equilibrium calculation of a simulated flue gas system containing 5%  $O_2$ , 10%  $CO_2$ , 15%  $H_2O$ , 200 ppm K, 100 ppm Cl and 200 ppm S (balanced by  $N_2$ ). The calculation is performed in FactSage 7.0, using the database of FactPS, FToxid, FTsalt and FTpulp.

Although the distribution of K species can be influenced by the molar ratios of K, Cl and S used in equilibrium calculations, the trend, that the formation of  $K_2SO_4$  is not

thermodynamically feasible at high temperatures (e.g. >1300 °C), exists generally. Thus, for high-temperature combustion systems, such as PF-fired boilers, the sulfation reactions can only happen at a certain temperature window, due to the thermodynamic restriction at high temperatures and the possible kinetic limitation at low temperatures. A further discussion of the kinetics of the sulfation reaction is provided in section 3.2.

It should be noted that the discussions above are only applicable to combustion systems with oxidizing condition. Under reducing condition, the thermodynamics of K-Cl-S system may change significantly, which is not addressed in this study.

### 3.2 Reaction of alkali species and sulfur additives

#### 3.2.1 Reaction with sulfur oxides

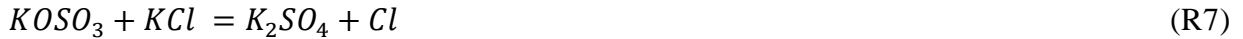
The reactions between alkali species (such as KCl and KOH) and gaseous sulfur oxides (SO<sub>2</sub> and SO<sub>3</sub>) can take place either in gas phase<sup>40-43</sup> or in condensed phase.<sup>44</sup> Within the short gas residence time in biomass-fired boilers, the gas-phase sulfation reaction usually plays a dominant role, while the condensed phase sulfation reaction is often more important for the alkali species deposited on boiler surfaces.

The gas-phase reaction between alkali species and sulfur oxides has been studied experimentally in flow reactors<sup>45,46</sup> and flame reactors.<sup>42</sup> Based on the experimental data, a detailed chemical kinetic model for gas-phase sulfation of alkali species has been developed by Glarborg et al.<sup>40-43</sup> The most updated model is presented in the work of Weng et al.<sup>43</sup> The model includes subsets for H<sub>2</sub> oxidation, sulfur chemistry, chlorine chemistry, alkali chemistry, and a simplified model describing the nucleation and condensation of gaseous K<sub>2</sub>SO<sub>4</sub>.<sup>42,43</sup>

Figure 2 shows the sulfation reaction pathways for a mixture of KCl (215 ppm) and SO<sub>2</sub> (245 ppm) at ~1200 K and ~900 K, respectively, downstream of a methane flame.<sup>43</sup> At ~1200 K, the main sulfation reaction pathway starts with the formation of atomic potassium from thermal dissociation of KCl. The formed the K atom is converted to KOSO<sub>3</sub>, through two pathways involving the reactions below:<sup>43</sup>



The KOSO<sub>3</sub> can further form K<sub>2</sub>SO<sub>4</sub> via two pathways involving the following reactions:<sup>43</sup>



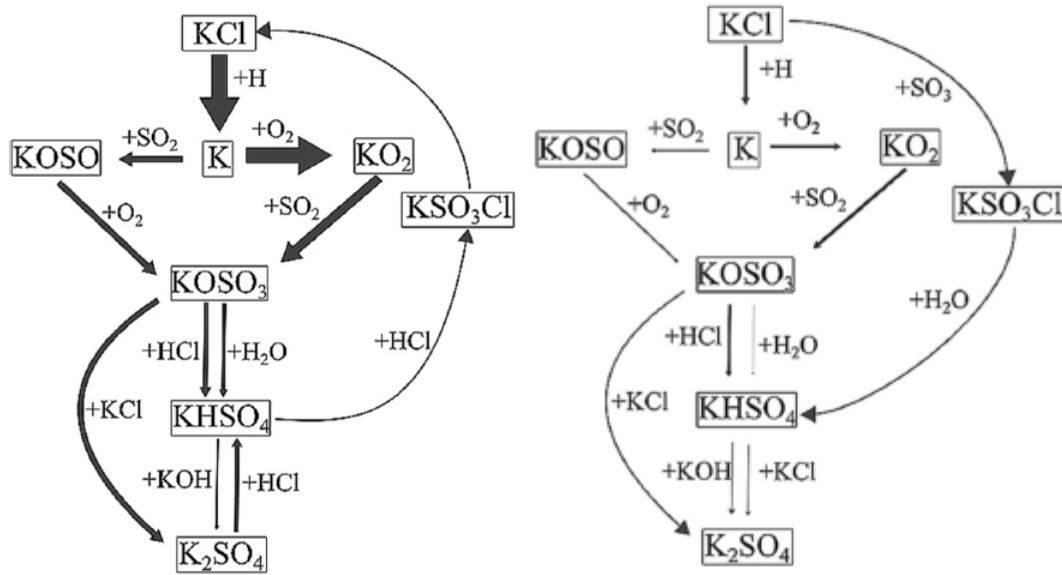


Figure 2 Reaction pathways for the formation of  $K_2SO_4$  from  $KCl$  (215 ppm) and  $SO_2$  (245 ppm) at  $\sim 1200$  K (left figure) and  $\sim 900$  K (right figure), downstream of a methane flame reactor with an equivalence ratio of 0.9. The line thickness indicates the significance of the reactions towards  $K_2SO_4$  formation.<sup>43</sup>

Compared to  $\sim 1200$  K, the pathways involving  $SO_3$  become important at  $\sim 900$  K, including:<sup>43</sup>



Sulfation of condensed phase  $KCl$  by  $SO_2$  has been studied experimentally in a thermogravimetric analyzer (TGA) and a fixed-bed reactor.<sup>44</sup> Based on the experiments, a simple model has been proposed to describe the condensed phase sulfation reaction of  $KCl$  by  $SO_2$ :<sup>44</sup>

$$\frac{dX}{dt} = 2.7 \times 10^7 \exp\left(-\frac{18900}{T}\right) (1-X)^{\frac{2}{3}} \frac{Y_{SO_2}}{1+708Y_{SO_2}} (Y_{O_2})^{0.37} \frac{R_0}{R_1} \quad (1)$$

### 3.2.2 Reaction with sulfates

Sulfate additives, including ammonium sulfate,<sup>19–24</sup> ferric sulfate,<sup>17,25</sup> aluminum sulfate,<sup>25</sup> have been shown to be effective in sulfation of gaseous alkali species in fluidized bed combustion and grate-combustion of biomass. The high effectiveness of sulfate additives is mainly related to the  $SO_3$  released during sulfate decomposition, which reacts with alkali chlorides and hydroxides significantly faster than  $SO_2$ .<sup>40–42</sup>

Thermal decomposition of ferric sulfate, aluminum sulfate and ammonium sulfate has been studied through TGA and fixed-bed experiments.<sup>47,48</sup> The sulfates produced both  $SO_2$  and  $SO_3$  during decomposition. At  $600$ – $900^\circ\text{C}$ , the ratio of the produced  $SO_3/SO_2$  from was around  $40/60$  and  $85/15$ , respectively, for ferric sulfate and aluminum sulfate decomposition. For ammonium sulfate, this ratio decreased with increasing decomposition temperature. Based on the experiments, a model describing the rate and product distribution of sulfate decomposition was

developed and combined with the chemical kinetic model of Li *et al.*<sup>42</sup> to describe the sulfation of alkali chlorides by sulfate additives.<sup>47,48</sup> The model was compared with biomass combustion experiments in a grate-firing reactor<sup>48,49</sup> and a bubbling fluidized bed reactor,<sup>47</sup> where ferric sulfate, ammonium sulfate, aluminum sulfate and elemental sulfur were used as additives.

The experimental and modeling results of alkali chlorides sulfation in a grate reactor firing a mixture of wood chips and corn stover with ferric sulfate and elemental sulfur additives are given in Figure 3. The results imply that the addition position has a significant influence on the effectiveness of ferric sulfate on sulfation of alkali chlorides. When ferric sulfate is injected to the grate, the effectiveness is much lower compared to the injection position at freeboard. This is because the  $\text{SO}_3$  released from ferric sulfate decomposition, before reacting with alkali chlorides, is nearly fully converted to  $\text{SO}_2$  at the high temperature zone ( $\sim 1100^\circ\text{C}$ ) above the grate. Thus, the effectiveness of ferric sulfate becomes similar to elemental sulfur. When the ferric sulfate is injected to the freeboard, less  $\text{SO}_3$  is converted to  $\text{SO}_2$  due the rapid cooling of the flue gas, and the presence of  $\text{SO}_3$  promotes the sulfation reaction, resulting in a much higher sulfation degree of the alkali chlorides. Another implication from Figure 3 is that when elemental sulfur is used as an additive, the sulfation degree of alkali chlorides is low, due to the kinetic restrictions that have been discussed in the chemical kinetic modeling work.<sup>40–43</sup>

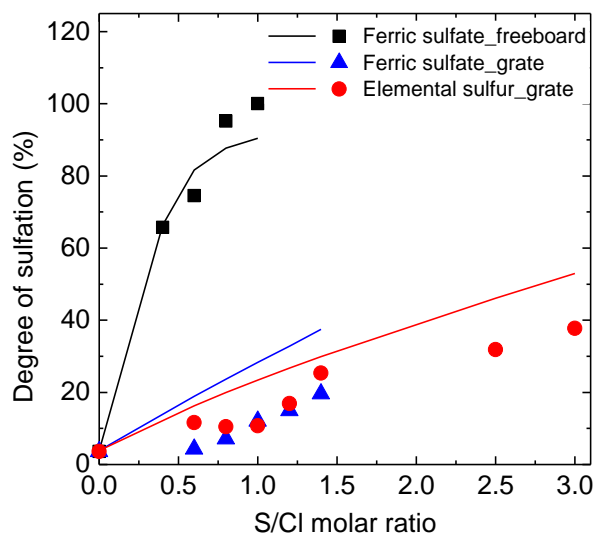


Figure 3 Experimental and simulated sulfation degree (%) of alkali chlorides ( $\sim 65$  ppmv) in a grate reactor firing a mixture of wood chips and corn stover.<sup>49</sup> The S/Cl molar ratio is calculated based on the sulfur in the additives and the chlorine in the fuel. Between the grate and the ferric sulfate injection position at the freeboard, the flue gas temperature is  $\sim 1050$ – $1100^\circ\text{C}$  and the residence time is  $\sim 1$ s. Downstream of the injection position at the freeboard, the flue gas temperature decreases from about  $1050^\circ\text{C}$  to  $600^\circ\text{C}$ , within a residence time of  $\sim 2$ s.<sup>49</sup>

### 3.3 Application of sulfur based additives in boilers

Utilization of sulfur based additives has been tested in biomass-fired fluidized bed and grate-firing boilers.<sup>15–18,20–25</sup> The observed effects of the sulfur based additives are summarized below:

- The concentrations of gaseous alkali chlorides in the flue gas are reduced, while the concentrations of HCl and SO<sub>2</sub> are increased.<sup>18,19</sup>
- The deposition rate on superheaters can either increase<sup>18,19</sup> or decrease.<sup>20,21,23</sup>
- In the deposits, the chlorine content is decreased, and the sulfur content is increased.<sup>18,20,21</sup> A reduction of the chlorine content in the deposits can mitigate the superheater corrosion.
- The chemistry and the size distribution of aerosols in the flue gas are changed.<sup>15,16,18,19,22</sup> The sulfur content is increased and the chlorine content is decreased in aerosols. The mass distribution of submicron aerosols often shifts towards larger diameters, possibly due to an increased degree of condensation.<sup>18,19</sup>

To the authors' knowledge, the use of sulfur based additives in PF-fired boilers has not been tested, partly related to the following challenges:

- In a PF-fired boiler, the gas residence time within the temperature window favored by the sulfation reaction may be rather limited.
- PF-boilers are typically equipped with a SCR unit, and sulfation of alkali chlorides to sulfates cannot completely address the SCR catalyst deactivation problems.

#### 4. ALUMINA-SILICATE ADDITIVES

The main working principle of Al-Si additives is the reaction between gaseous alkali chlorides and the Al-Si additives, forming alkali aluminosilicates and hydrogen chloride. Compared to alkali chlorides, the melting temperatures of alkali aluminosilicates are much higher. Thus, the reaction can lead to a reduced deposit formation and/or more easily removable deposits in boilers. The conversion of alkali chlorides to hydrogen chloride reduces the corrosion risks in boilers. Deactivation of catalyst in the SCR units can also be mitigated, because alkali aluminosilicates are less chemically aggressive than alkali chlorides, and they often exist as relatively large particles that are less likely to cause physical blocking of the SCR catalyst compared to the submicron aerosols generated from gaseous alkali species.

##### 4.1 Thermodynamics of Si-Al-K-Cl system

The thermodynamics of a typical Si-Al-K-Cl system is evaluated through global equilibrium calculations of a simulated flue gas containing 5% O<sub>2</sub>, 10% CO<sub>2</sub>, 15% H<sub>2</sub>O, 200 ppm K, 100 ppm Cl, 200 ppm Si and 200 ppm Al (balanced by N<sub>2</sub>). The distribution of the K species in the temperature range of 600-1500 °C is shown in Figure 4. At temperatures above 1300 °C, different from the K-S-Cl system (Figure 1) where KOH (g) and KCl (g) are the only thermodynamically favorable K species, 50% of the potassium exists as KAlSi<sub>2</sub>O<sub>6</sub>. When the temperature decreases to ~1220 °C, KAlSiO<sub>4</sub> is formed and the amount of KAlSiO<sub>4</sub> is increased with decreasing temperatures. At ~600 °C, KAlSiO<sub>4</sub> is the only thermodynamically favorable potassium species under the current conditions.

The results in Figure 4 imply that the formation of potassium aluminosilicates is thermodynamically favorable at high temperatures. Typically, the reaction rate of gaseous alkali species and aluminosilicates is also higher with increasing temperatures. Thus, the application of



Al-Si additives may be more effective in combustion systems with high temperatures, such as PF-fired boilers.

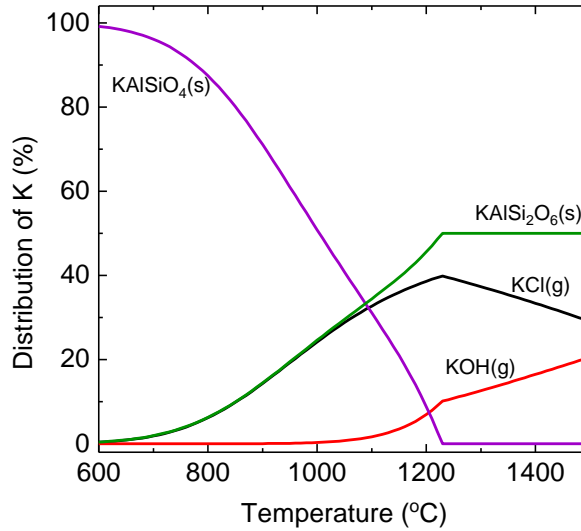


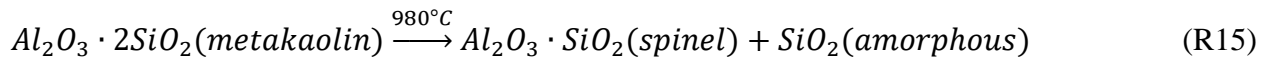
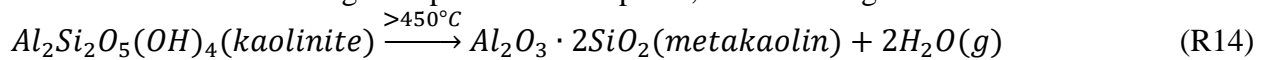
Figure 4 Distribution of K species from global equilibrium calculation of a simulated flue gas system containing 5% O<sub>2</sub>, 10% CO<sub>2</sub>, 15% H<sub>2</sub>O, 200 ppm K, 100 ppm Cl, 200 ppm Si and 200 ppm Al (balanced by N<sub>2</sub>). The calculation is performed in FactSage 7.0, with the database of FactPS, FToxid, FTSalt and FTpulp.

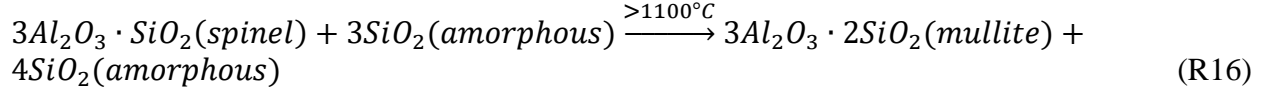
## 4.2 Reaction of alkali species and Al-Si additives

### 4.2.1 Reaction with kaolin

Kaolin, mainly comprised of kaolinite (Al<sub>2</sub>Si<sub>2</sub>O<sub>5</sub>(OH)<sub>4</sub>), is one of the most effective Al-Si additives for capturing gaseous alkali species. The reaction between kaolin and gaseous alkali species has been studied experimentally in fixed-bed reactors<sup>32,36,50</sup> and in flow reactors.<sup>28–31</sup> The kaolin particles used in fixed bed reactors are usually of millimeter size, with particle residence time in an order of hours.<sup>32,36,50</sup> The fixed-bed experiments can provide insights into the reaction mechanism. However, it is not straightforward to use directly the results to evaluate the performance of kaolin additives in biomass combustion, since the kaolin additives are usually in micrometer size range and the residence time is typically in seconds.<sup>18,27,33</sup> In flow reactors, the kaolin particles used are usually of a size of a few micrometers and the particle residence time is in an order of seconds,<sup>28–31</sup> which mimic the application conditions better.

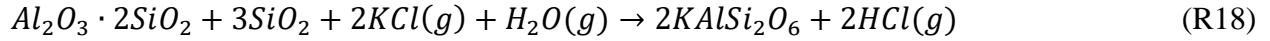
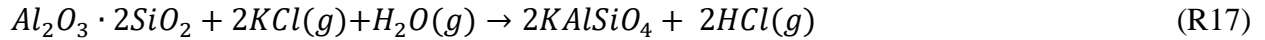
When kaolin enters a high temperature atmosphere, the following reactions can occur:<sup>32</sup>





Calcination of micrometer-size kaolin particles has been studied in an entrained flow reactor at a temperature of 1300 °C and a gas residence time of 1.2s.<sup>30</sup> No kaolinite was detected in the solid product, indicating that R14 was completed. Mullite and quartz were detected in the product. A comparison with the fully calcined kaolin particles revealed that only a fraction of the kaolin was converted to mullite in the reactor at 1300 °C, with the remaining existing in amorphous phase, e.g. as metakaolin and spinel. However, at 900 °C and a gas residence time of 1.2s, kaolinite was detected in the product, indicating that R14 was not completed.<sup>30</sup>

Most of the products from kaolin calcination are reactive towards gaseous alkali species. As an example, the reactions between KCl and metakaolin are given below:



The  $KAlSiO_4$  can be either kalsilite or kaliophilite, while  $KAlSi_2O_6$  is leucite. Similar reactions as R17 and R18 also occur between metakaolin and KOH.<sup>30</sup> Moreover, mullite<sup>30-32</sup> and  $SiO_2$ <sup>51</sup> can also be reactive towards gaseous alkali species.

The findings regarding the reaction between kaolin and gaseous alkali species in fixed bed reactors<sup>32,36,50,52</sup> are summarized below:

- Millimeter-size kaolin flakes reacted with gaseous NaCl (230 ppm) at 800 °C with the presence of water vapor (2%), forming  $NaAl_2Si_2O_8$  (nephelite and carnegieite).<sup>36</sup>
- For millimeter-size kaolin pellets placed in a gas atmosphere with oxygen and water vapor,<sup>32</sup> the reaction rate between KCl (g) and kaolin decreased when the reactor temperature was increased from 900 to 1300 °C, explained by an increased degree of sintering limiting the diffusion of KCl (g). The diffusion limitation was supported by SEM-EDX analysis of the reacted particles at 900 °C, showing that only the outer part was reacted. When the temperature was increased from 1300 to 1500 °C, an increased reaction rate was observed, explained by the formation of melt in the pellets which improved the transport of KCl through liquid phase diffusion. The reaction rate was not influenced by the oxygen concentration, and the effect of water vapor concentration became negligible when it was above 1%.<sup>32</sup>
- For millimeter-size kaolin particles in a fixed-bed reactor with a temperature of 750-960 °C and a KCl concentration varying of 0.01-1.1ppm,<sup>50</sup> less KCl was captured by kaolin particles with an increasing temperature and a decreasing KCl concentration. The effect of temperature was consistent with the trend obtained in equilibrium calculations.<sup>50</sup> Under an air atmosphere at 850 °C, kaolin captured KCl slightly more effectively than KOH, while  $K_2SO_4$  was captured much less effectively than KCl.<sup>50</sup> Under reducing conditions, KOH was captured more effectively than KCl.<sup>52</sup>

The reaction between kaolin and gaseous alkali species has been studied in flow reactors by Mwabe et al.<sup>28</sup>, Gale et al.<sup>29</sup> and Wang et al.<sup>30,31</sup> Figure 5 shows the conversion of different alkali

species to alkali aluminosilicates under different kaolin/alkali dosage conditions, represented by the molar ratio of alkali/Si fed to the reactor.<sup>29–31</sup> The experiments were performed under temperature conditions of 1300–1100 °C and gas residence time of 0.8–1.2s, simulating the conditions of PF boilers. The results show that KOH and K<sub>2</sub>CO<sub>3</sub> have similar conversion, and no significant difference is observed at 1300 and 1100°C. The similarity between K<sub>2</sub>CO<sub>3</sub> and KOH is attributed to a rapid conversion of K<sub>2</sub>CO<sub>3</sub> to KOH in the reactor.<sup>31</sup> When the alkali/Si molar ratio increases from about 0.1 to 1.8, the conversion of KOH/K<sub>2</sub>CO<sub>3</sub> decreases from approximately 95% to 40%, primarily due to a change of the thermodynamics of the system.<sup>30,31</sup> Compared to KOH/K<sub>2</sub>CO<sub>3</sub>, the conversion of KCl and K<sub>2</sub>SO<sub>4</sub> is considerably lower. The inhibition effect of chlorine and SO<sub>2</sub> on NaOH and kaolin reactions has also been observed by Mwabe et al.<sup>28</sup> Compared to KOH/K<sub>2</sub>CO<sub>3</sub>, the conversion of sodium acetate, which converts rapidly to NaOH upon injection,<sup>29</sup> is similar at an alkali/Si molar ratio of ~1. However, with higher alkali/Si molar ratios, the conversion of sodium acetate becomes much higher than that of KOH/K<sub>2</sub>CO<sub>3</sub>. The different behaviors of the sodium species and potassium may be related to the differences in experimental conditions and methods,<sup>29–31</sup> which needs to be further evaluated.

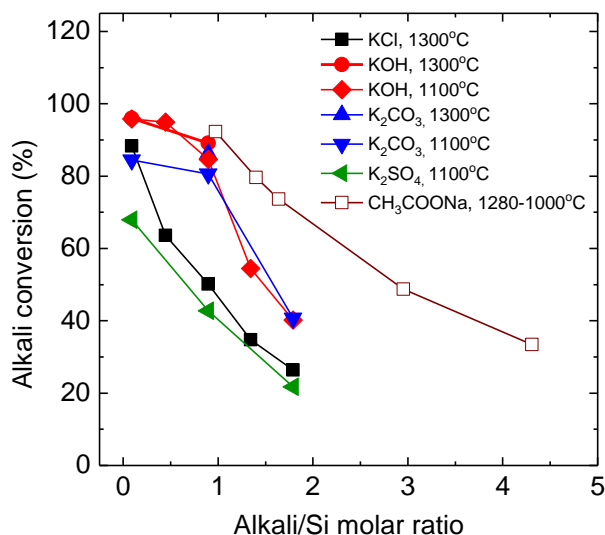


Figure 5 Conversion of gaseous alkali species to alkali aluminosilicates in flow reactors, under different kaolin/alkali dosage conditions, represented by the molar ratio of alkali/Si fed to the reactor.<sup>29–31</sup> The experiments of the potassium species were conducted in an electrical heated entrained flow reactor with a gas residence time of ~1.2s. A slurry containing kaolin particles ( $D_{50}=5.47\ \mu\text{m}$ ) and potassium aqueous solution was injected to the reactor.<sup>30,31</sup> The experiments related to the sodium were performed in a laminar flow combustor firing nature gas, with sodium acetate solution injected to the burner via a atomizer, kaolin particles of ~2  $\mu\text{m}$  added at a location with a gas temperature of 1280/1160°C, and the product sampled at ~1000°C. The gas residence time between the kaolin injection position and the particle sampling position was 1.15–0.84s.<sup>29</sup>

Figure 6 shows the influence of reactor temperature on the conversion of KOH to potassium aluminosilicates. For a low K/Si molar ratio of  $\sim 0.1$ , the effect of temperature is insignificant. However, when the K/Si molar ratio is  $\sim 1$ , temperature influences the conversion considerably. The highest conversion is obtained at 1100-1300°C. Increasing the temperature further to 1450°C results in a decreased conversion, which is explained by a change of reaction product from  $\text{KAlSiO}_4$  to  $\text{KAlSi}_2\text{O}_6$  based on thermodynamic calculations.<sup>30</sup> The relatively low conversion at 900 and 800 °C is attributed to kinetic limitations and that part of the added KOH may not be fully vaporized in the reactor.<sup>30</sup>

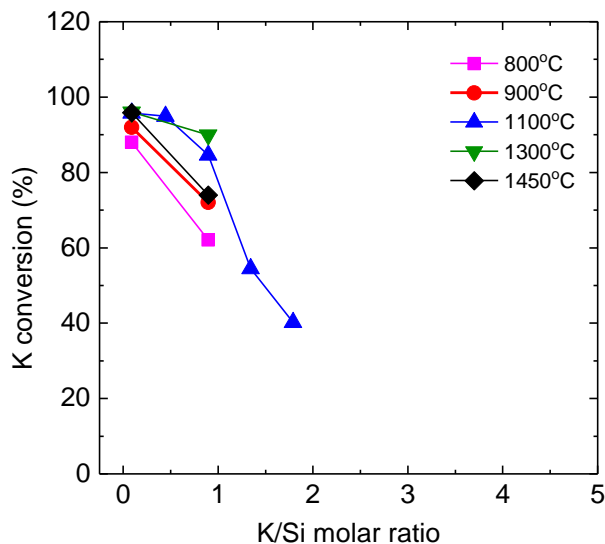


Figure 6 Conversion of KOH to potassium aluminosilicates by kaolin addition in an entrained flow reactor under different temperature and KOH dosage (represented by the molar ratio of K/Si fed to the reactor) conditions.<sup>30,31</sup> The experiments were conducted with a gas residence time of  $\sim 1.2$ s and a slurry containing kaolin particles ( $D_{50}=5.47 \mu\text{m}$ ) and KOH aqueous solution.<sup>30,31</sup>

The influence of kaolin particle size ( $D_{50}=3.51, 5.47, 13.48\mu\text{m}$ ) on the conversion of KOH has been evaluated in the entrained flow reactor at a K/Si molar ratio of  $\sim 0.9$ , a gas residence time of  $\sim 1.2$ s, and reactor temperatures of 900-1300 °C.<sup>30</sup> The conversion for particles with  $D_{50}=3.51 \mu\text{m}$  and  $5.47 \mu\text{m}$  was almost identical, while a slightly ( $\sim 10\%$ ) lower conversion was obtained for the particles with  $D_{50}=13.48 \mu\text{m}$  at 1100-1300 °C, implying a transport limitation for the large kaolin particles. The impact of the gas residence time (0.7-1.9s) has been studied at a K/Si molar ratio of  $\sim 0.9$  and a temperature of 1100 °C. The conversion was increased slightly ( $\sim 10\%$ ) when the residence time was increased from 0.7s to 1.9s, implying a small influence of the residence time and that the reaction took place fast in the reactor.<sup>30,31</sup>

Figure 7 compares the equilibrium and experimental conversion of different potassium species reacting with kaolin particles ( $D_{50}=5.47 \mu\text{m}$ ) in an entrained flow reactor at a temperature of 1100-1450 °C and a gas residence time of  $\sim 1.2$ s. The experimental conversion does not exceed the equilibrium conversion. For KOH,  $\text{K}_2\text{CO}_3$  and KCl, the experimental conversion is quite close to the equilibrium conversion, with most of them lay within 20% deviation. This implies

that the reactions between kaolin and these potassium species are fast under the experimental conditions, and that the chosen equilibrium model represents well the experimental systems containing KOH, K<sub>2</sub>CO<sub>3</sub> and KCl. However, for K<sub>2</sub>SO<sub>4</sub>, a significant deviation exists between the experimental conversion and the equilibrium conversion. This may be because the equilibrium model does not present well the experimental system containing K<sub>2</sub>SO<sub>4</sub>, e.g. due to uncertainties of the thermodynamic data of sulfur species. Experimental uncertainties, e.g. slow or incomplete vaporization/decomposition of K<sub>2</sub>SO<sub>4</sub> in the reactor, may also contribute to this discrepancy. Further work is needed in order to understand the behavior of the K<sub>2</sub>SO<sub>4</sub> and kaolin system.

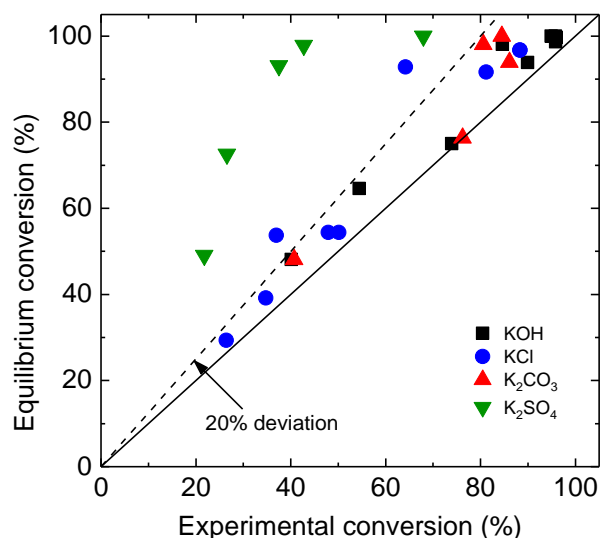


Figure 7 A comparison of the experimental and equilibrium conversion of different potassium species with kaolin addition. The experiments were conducted in an entrained flow reactor with a temperature of 1100-1450 °C, a gas residence time of ~1.2s and a slurry containing kaolin particles ( $D_{50}=5.47\ \mu\text{m}$ ) and aqueous solution of the potassium species (K/Si molar ratio of ~0.1-1.8).<sup>30,31</sup> The equilibrium conversion was obtained from global equilibrium calculation in FactSage 7.0, using the database of FactPS, FToxid, FTsalt and FTpulp.<sup>30,31</sup>

#### 4.2.1 Reaction with other Al-Si additives

The reaction between gaseous alkali species and other Al-Si additives, including coal ash, silica, mullite and emahlite, has been studied through fixed-bed experiments.<sup>32,36,53</sup> The results from Zheng et al.<sup>32</sup>, where millimeter-size additive pellets were placed in a gas atmosphere containing KCl (g), oxygen and water vapor for a few hours, are summarized below:

- Mullite pellets were not reactive towards KCl (g) at 1200 °C or below. This was explained by a high degree of sintering occurred during the preparation of the mullite pellets, which limited the diffusion KCl (g) into the pellets. At 1300 °C, the mullite pellets started to react with KCl (g), and the reaction rate increased with increasing temperatures. This was explained by the formation of a molten phase at 1300 °C and higher temperatures, which promoted the diffusion of KCl (g) and thereby its reaction with mullite pellets.

- Bituminous coal ash pellets were reactive towards KCl (g) in the temperature range of 900-1300 °C. The reaction rate decreased with an increasing reactor temperature from 900 to 1200 °C, while the reaction rate increased when the temperature was increased from 1200 to 1300°C. The potassium capture capability of the coal ash pellet was comparable to that of kaolin pellet.
- Silica pellets were not reactive toward KCl (g) in the temperature range of 900-1500 °C.

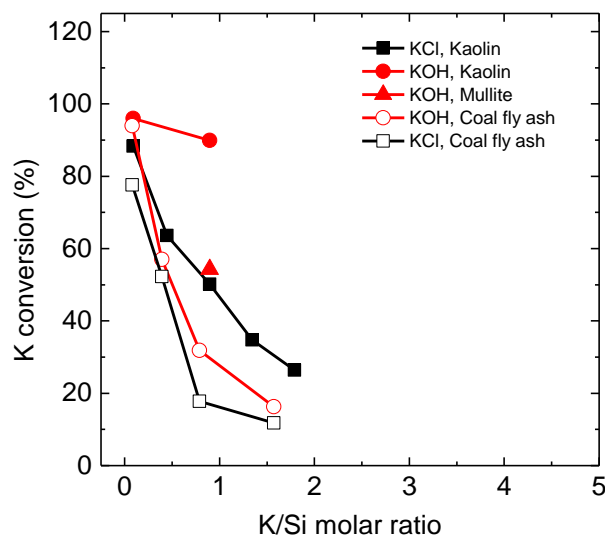


Figure 8 Conversion of KOH and KCl to potassium aluminosilicates by kaolin ( $D_{50}=5.47 \mu\text{m}$ ), mullite ( $D_{50}=5.90 \mu\text{m}$ ), and coal fly ash ( $0-32 \mu\text{m}$ , from Asnæs Power Station) addition in an entrained flow reactor under different K-dosage (represented by the molar ratio of K/Si fed to the reactor) conditions. The experiments were conducted at 1300 °C and a gas residence time of ~1.2s.<sup>30,31,53</sup>

Figure 8 compares the effect of kaolin, mullite and a coal fly ash on KCl and KOH capture in a flow reactor with a gas residence time of 1.2s and a temperature of 1300 °C.<sup>30,31,53</sup> The capture efficiency decreases in an order of kaolin, mullite and the coal fly ash. However, at K/Si molar ratio of ~0.1, kaolin and the coal fly ash has a similar effectiveness towards KOH capture. Compared to KOH, the KCl is less effectively captured by coal fly ash.

Figure 9 shows the equilibrium and experimental conversion of KOH and KCl reacting with coal fly ash ( $0-32 \mu\text{m}$ , from Asnæs Power Station) in an entrained flow reactor at a temperature of 1100-1450 °C and a gas residence time of ~1.2s. The experimental conversion is generally much lower than that predicted by equilibrium calculation. The only data points that lay within 20% deviation of the equilibrium conversion are from the experiments with a K/Si molar of ~0.1, where a significant excess amount of coal fly ash is available for potassium capture. The significant deviation in Figure 9 implies that the reaction between coal fly ash and KCl/KOH is possibly kinetic and/or transport limited. Further work, including modeling study, is needed in order to understand and predict the behavior of coal fly ash on alkali capture.

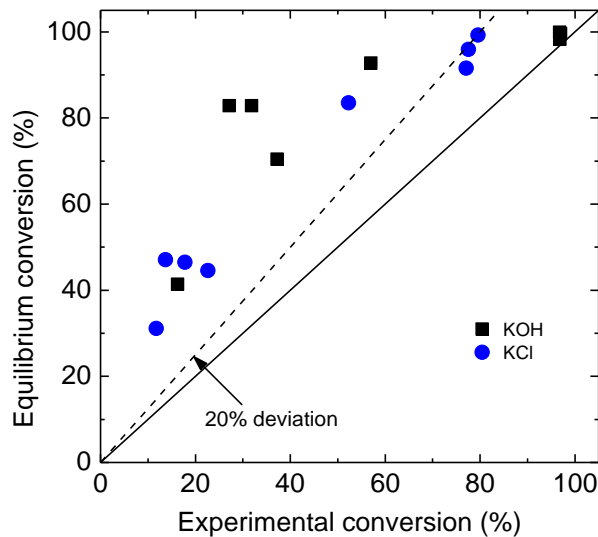


Figure 9 A comparison of the experimental and equilibrium conversion of KOH and KCl with coal fly ash (0-32  $\mu\text{m}$ , from Asnæs Power Station) addition. The experiments were conducted in an entrained flow reactor with a temperature of 1100-1450  $^{\circ}\text{C}$ , a gas residence time of  $\sim 1.2\text{s}$  and a K/Si molar ratio of  $\sim 0.1\text{-}1.6$ .<sup>30,31</sup> The equilibrium conversion was obtained from global equilibrium calculation in FactSage 7.0, using the database of FactPS, FToxid, FTsalt and FTpulp.<sup>30,31</sup>

#### 4.3 Application of Al-Si additives in biomass boilers

Coal fly ash is used as an additive in several wood-fired PF boilers in Denmark. The effects of coal fly ash addition on aerosol formation and ash deposition in a 800MW<sub>th</sub> wood-fired PF boiler have been studied through full-scale measurements,<sup>7,8</sup> and are summarized below:

- Addition of about 6 ton/h coal fly ash to 130-140 ton/h pulverized wood pellets firing reduced the mass-load of submicron particles from about 44-47 mg/Nm<sup>3</sup> to 11-19 mg/Nm<sup>3</sup>. And the composition of the submicron particles was changed from K-Cl-S rich to Ca-P-Si rich.<sup>8</sup>
- With the addition of coal fly ash, the deposits formed at a flue gas temperature of 1300  $^{\circ}\text{C}$  became easily removal, and the deposit composition was changed to be Al-Si rich with a negligible amount of alkali sulfates, chlorides and hydroxides. For the deposits formed at a flue gas temperature of 800  $^{\circ}\text{C}$ , KCl disappeared in the deposits when coal fly ash was added. The K<sub>2</sub>SO<sub>4</sub>, KCl, KOH and K<sub>2</sub>CO<sub>3</sub> in the fly ash collected by electrostatic precipitator (ESP) disappeared when coal fly ash was added.<sup>7</sup>

Kaolin has also been tested as an additive in a biomass-fired fluidized bed boiler.<sup>18</sup> The addition of kaolin reduced the gaseous alkali chlorides concentration in the flue gas, increased the agglomeration temperature of bed materials, and decreased the chlorine content in the deposits. However, one of the main challenges regarding using kaolin is its high materials cost.<sup>18</sup>

## 5. CONCLUSIONS

The current understanding and applications of sulfur based additives and Al-Si based additives in biomass combustion have been reviewed. A detailed chemical kinetic model describing the gaseous sulfation of alkali chlorides by sulfur oxides and different sulfates has been available. The sulfur based additives are mainly applied in fluidized bed and grate firing boilers, and are primarily based on sulfates that can produce  $\text{SO}_3$  upon decomposition. Kaolin is the most studied Al-Si additives. Micrometer-size kaolin particles can react rapidly with KOH and KCl under PF-boiler conditions, with the conversion being close to chemical equilibrium. Coal fly ash, although less reactive than kaolin, has been applied commercially in PF-boilers firing wood pellets to address the ash deposition, corrosion and SCR catalyst deactivation problems.

## ACKNOWLEDGMENT

The work is part of the CHEC (Combustion and Harmful Emission Control) research program. The authors would like to thank the financial support of the Danish Strategic Research Council (GREEN), the 'Flexible use of Biomass on PF fired power plants' project funded by Energinet through the ForskEL program, Ørsted and Technical University of Denmark (DTU), and the advanced technology platform 'Minerals and Cement Process Technology-MiCeTech' funded by the Innovation Fund Denmark, FLSmidt A/S, Hempel and DTU (Grant No. 39-2013-2).

## REFERENCES

- (1) Hansen, S. B.; Jensen, P. A.; Frandsen, F. J.; Wu, H.; Bashir, M. S.; Wadenbäck, J.; Sander, B.; Glarborg, P. *Energy Fuels* **2014**, 28 (6), 3539–3555.
- (2) Zheng, Y.; Jensen, A. D.; Johnsson, J. E. *Appl. Catal. B Environ.* **2005**, 60 (3–4), 253–264.
- (3) Lin, W.; Dam-Johansen, K.; Frandsen, F. *Chem. Eng. J.* **2003**, 96 (1–3), 171–185.
- (4) Knudsen, J. N.; Jensen, P. A.; Dam-Johansen, K. *Energy Fuels* **2004**, 18 (5), 1385–1399.
- (5) Bashir, M. S.; Jensen, P. A.; Frandsen, F.; Wedel, S.; Dam-Johansen, K.; Wadenbäck, J.; Pedersen, S. T. *Fuel Process. Technol.* **2012**, 97, 93–106.
- (6) van Lith, S. C.; Jensen, P. A.; Frandsen, F. J.; Glarborg, P. *Energy Fuels* **2008**, 22 (3), 1598–1609.
- (7) Wu, H.; Bashir, M. S.; Jensen, P. A.; Sander, B.; Glarborg, P. *Fuel* **2013**, 113, 632–643.
- (8) Damø, A. J.; Wu, H.; Frandsen, F. J.; Glarborg, P.; Sander, B. *Energy Fuels* **2014**, 28 (5), 3217–3223.
- (9) Zheng, Y.; Jensen, P. A.; Jensen, A. D.; Sander, B.; Junker, H. *Fuel* **2007**, 86 (7–8), 1008–1020.
- (10) Jensen, P. A.; Sander, B.; Dam-Johansen, K. *Biomass Bioenergy* **2001**, 20 (6), 447–457.
- (11) Saleh, S. B.; Flensburg, J. P.; Shoulaifar, T. K.; Sárossy, Z.; Hansen, B. B.; Egsgaard, H.; Demartini, N.; Jensen, P. A.; Glarborg, P.; Dam-Johansen, K. *Energy Fuels* **2014**, 28 (6), 3738–3746.
- (12) Jensen, P. A.; Frandsen, F. J.; Wu, H.; Glarborg, P. A Review: Fly Ash and Deposit Formation in PF Fired Biomass Boilers. In *Impacts of Fuel Quality on Power Production*; 2016.
- (13) Sippula, O.; Lind, T.; Jokiniemi, J. *Fuel* **2008**, 87 (12), 2425–2436.



- (14) Jiménez, S.; Ballester, J. *Combust. Flame* **2005**, *140* (4), 346–358.
- (15) Lind, T.; Kauppinen, E. I.; Hokkinen, J.; Jokiniemi, J. K.; Orjala, M.; Aurela, M.; Hillamo, R. *Energy Fuels* **2006**, *20* (1), 61–68.
- (16) Davidsson, K. O.; Åmand, L. E.; Leckner, B.; Kovacevik, B.; Svane, M.; Hagström, M.; Pettersson, J. B. C.; Petterson, J.; Asteman, H.; Svensson, J. E.; et al. *Energy Fuels* **2007**, *21* (1), 71–81.
- (17) Aho, M.; Paakkinen, K.; Taipale, R. *Fuel* **2013**, *103*, 562–569.
- (18) Davidsson, K. O.; Åmand, L. E.; Steenari, B. M.; Elled, A. L.; Eskilsson, D.; Leckner, B. *Chem. Eng. Sci.* **2008**, *63* (21), 5314–5329.
- (19) Kassman, H.; Båfver, L.; Åmand, L. E. *Combust. Flame* **2010**, *157* (9), 1649–1657.
- (20) Kassman, H.; Pettersson, J.; Steenari, B. M.; Åmand, L. E. Two Strategies to Reduce Gaseous KCl and Chlorine in Deposits during Biomass Combustion - Injection of Ammonium Sulphate and Co-Combustion with Peat. In *Fuel Processing Technology*; 2013; Vol. 105, pp 170–180.
- (21) Kassman, H.; Broström, M.; Berg, M.; Åmand, L. E. *Fuel* **2011**, *90* (4), 1325–1334.
- (22) Zeuthen, J. H.; Jensen, P. A.; Jensen, J. P.; Livbjerg, H. *Energy Fuels* **2007**, *21* (2), 699–709.
- (23) Kassman, H.; Normann, F.; Åmand, L. E. *Combust. Flame* **2013**, *160* (10), 2231–2241.
- (24) Broström, M.; Kassman, H.; Helgesson, A.; Berg, M.; Andersson, C.; Backman, R.; Nordin, A. *Fuel Process. Technol.* **2007**, *88* (11–12), 1171–1177.
- (25) Aho, M.; Vainikka, P.; Taipale, R.; Yrjas, P. *Fuel* **2008**, *87* (6), 647–654.
- (26) Andersson, S.; Blomqvist, E. W.; Bafver, L.; Jones, F.; Davidsson, K.; Froitzheim, J.; Karlsson, M.; Larsson, E.; Liske, J. *Waste Manag.* **2014**, *34* (1), 67–78.
- (27) Wu, H.; Glarborg, P.; Frandsen, F. J.; Dam-Johansen, K.; Jensen, P. A. *Energy Fuels* **2011**, *25* (7).
- (28) Mwabe, P. O.; Wendt, J. O. L. *Proc. Combust. Inst.* **1996**, *26* (2), 2447–2453.
- (29) Gale, T. K.; Wendt, J. O. L. *Combust. Flame* **2002**, *131* (3), 299–307.
- (30) Wang, G.; Jensen, P. A.; Wu, H.; Frandsen, Flemming Jappe; Sander, B.; Glarborg, P. *Energy Fuels* **2018**, *32* (2), 1851–1862.
- (31) Wang, G.; Jensen, P. A.; Wu, H.; Frandsen, F. J.; Sander, B.; Glarborg, P. *Energy Fuels* **2018**, *32* (3), 3566–3578.
- (32) Zheng, Y.; Jensen, P. A.; Jensen, A. D. *Fuel* **2008**, *87* (15–16), 3304–3312.
- (33) Aho, M. *Fuel* **2001**, *80* (13), 1943–1951.
- (34) Coda, B.; Aho, M.; Berger, R.; Hein, K. R. G. *Energy Fuels* **2001**, *15* (3), 680–690.
- (35) Tobiasen, L.; Skytte, R.; Pedersen, L. S.; Pedersen, S. T.; Lindberg, M. A. *Fuel Process. Technol.* **2007**, *88* (11–12), 1108–1117.
- (36) Uberoi, M.; Punjak, W. A.; Shadman, F. *Prog. Energy Combust. Sci.* **1990**, *16* (4), 205–211.
- (37) Novaković, A.; Van Lith, S. C.; Frandsen, F. J.; Jensen, P. A.; Holgersen, L. B. *Energy Fuels* **2009**, *23* (7), 3423–3428.
- (38) Almark, M.; Edvardsson, E.; Berg, M. Reductoin of Alkali Chlorides in Flue Gas and Chloirine in Deposits by Phosphate Addition. In *Impacts of Fuel Quality on Power Generation and the Envrionment*; 2010.
- (39) Olsen, B. K.; Kügler, F.; Castellino, F.; Jensen, A. D. *Catal. Sci. Technol.* **2016**, *6*, 2249–2260.
- (40) Glarborg, P.; Marshall, P. *Combust. Flame* **2005**, *141* (1–2), 22–39.

- (41) Hindiyarti, L.; Frandsen, F.; Livbjerg, H.; Glarborg, P.; Marshall, P. *Fuel* **2008**, 87 (8–9), 1591–1600.
- (42) Li, B.; Sun, Z.; Li, Z.; Aldén, M.; Jakobsen, J. G.; Hansen, S.; Glarborg, P. *Combust. Flame* **2013**, 160 (5), 959–969.
- (43) Weng, W.; Chen, S.; Wu, H.; Glarborg, P.; Li, Z. *Fuel* **2018**, 224, 461–468.
- (44) Sengeløv, L. W.; Hansen, T. B.; Bartolome, C.; Wu, H.; Pedersen, K. H.; Frandsen, F. J.; Jensen, A. D.; Glarborg, P. *Energy Fuels* **2013**, 27, 3283–3289.
- (45) Iisa, K.; Lu, Y.; Salmenoja, K. *Energy Fuels* **1999**, 13 (6), 1184–1190.
- (46) Jensen, J. R.; Nielsen, L. B.; Schultz-Møller, C.; Wedel, S.; Livbjerg, H. *Aerosol Sci. Technol.* **2000**, 33 (6), 490–509.
- (47) Wu, H.; Pedersen, M. N.; Jespersen, J. B.; Aho, M.; Roppo, J.; Frandsen, F. J.; Glarborg, P. *Energy Fuels* **2014**, 28 (28), 199–207.
- (48) Wu, H.; Jespersen, J. B.; Frandsen, F. J.; Glarborg, P.; Aho, M.; Paakkinen, K.; Taipale, R. *AIChE J.* **2013**, 59 (11), 4314–4324.
- (49) Wu, H.; Jespersen, J. B.; Aho, M.; Paakkinen, K.; Taipale, R.; Frandsen, F. J.; Glarborg, P. Modeling of Sulfation of Potassium Chloride by Ferric Sulfate Addition during Grate-Firing of Biomass. In *Finnish-Swedish Flame Days*; 2013.
- (50) Tran, K. Q.; Iisa, K.; Steenari, B. M.; Lindqvist, O. *Fuel* **2005**, 84 (2–3), 169–175.
- (51) Wibberley, L. J.; Wall, T. F. *Fuel* **1982**, 61, 93–99.
- (52) Tran, Q. K.; Steenari, B. M.; Iisa, K.; Lindqvist, O. *Energy Fuels* **2004**, 18, 1880–1876.
- (53) Wang, G. Potassium Capture by Kaolin and Coal Fly Ash. PhD Thesis, Technical University of Denmark, 2018.